

# Experimental demonstration of a Hadamard gate for coherent state qubits

Anders Tipsmark,<sup>1,\*</sup> Ruifang Dong,<sup>2,1</sup> Amine Laghaout,<sup>1</sup> Petr Marek,<sup>3</sup> Miroslav Ježek,<sup>3,1</sup> and Ulrik L. Andersen<sup>1</sup>

<sup>1</sup>*Department of Physics, Technical University of Denmark, Fysikvej, 2800 Kgs. Lyngby, Denmark*

<sup>2</sup>*Quantum Frequency Standards Division, National Time Service Center (NTSC),*

*Chinese Academy of Sciences, 710600 Lintong, Shaanxi, China*

<sup>3</sup>*Department of Optics, Palacký University, 17. listopadu 12, 77146 Olomouc, Czech Republic*

(Dated: April 13, 2022)

We discuss and experimentally demonstrate a probabilistic Hadamard gate for coherent state qubits. The scheme is based on linear optical components, non-classical resources and the joint projective action of a photon counter and a homodyne detector. We experimentally characterize the gate for the coherent states of the computational basis by full tomographic reconstruction of the transformed output states. Based on the parameters of the experiment we simulate the fidelity for all coherent state qubits on the Bloch sphere.

PACS numbers: 03.67.-a, 03.67.Lx, 42.50.Ex

Measurement-based, linear optical quantum processors rely on off-line prepared resources, linear optical transformations and measurement-induced operations [1]. Among all measurement-based protocols, the most famous ones are the cluster state quantum processor where universal operations are executed by measuring a large entangled cluster state [2], and the linear quantum computer approach proposed by Knill, Laflamme, and Milburn [3]. The latter method is based on single photon resources that interfere in a linear optical network and subsequently are measured to enforce the desired operation. Despite its seeming simplicity, the implementation of a fault tolerant operating algorithm is complex as it requires a very large overhead.

An alternative approach to measurement based linear quantum computing has been put forward by Ralph *et al.* [4]. Rather than using discrete degrees of freedom (e.g. the polarization) of a single photon as the computational basis, it was suggested to use two mesoscopic coherent states,  $|\alpha\rangle$  and  $|-\alpha\rangle$ , where  $\alpha$  is the amplitude. Although these states are only approximately orthogonal ( $\langle\alpha|-\alpha\rangle \neq 0$ ), resource efficient and fault tolerant quantum gates can be implemented: For a large coherent amplitude, that is  $\alpha > 2$ , deterministic gates can in principle be realized although the experimental implementation is very challenging [5]. On the other hand, by employing a simpler physical implementation, non-deterministic gates can be realized for any value of  $\alpha$ , and for  $\alpha > 1.2$ , the scheme was theoretically shown to be fault-tolerant and resource efficient [6].

An even simpler implementation of a universal set of non-deterministic quantum gates was recently suggested by Marek and Fiurášek [7]. They proposed the physical realization of a single mode and a two-mode phase gate as well as the Hadamard gate. In this Letter we present a proof of principle experiment of the probabilistic Hadamard gate for coherent state qubits. The implemented protocol is based on a squeezed state resource, linear operations as well as two projective measurements

of discrete and continuous variables. By injecting the computational basis states ( $|\alpha\rangle$  and  $|-\alpha\rangle$ ) into the gate we characterize its function by reconstructing the Wigner functions of the transformed output states and calculate the fidelity with ideally transformed state. The implementation of the Hadamard gate demonstrated in this Letter constitutes the very first step towards the realization of a quantum processor based on coherent state qubits.

A Hadamard gate transforms the computational basis states,  $|\pm\alpha\rangle$ , into the diagonal basis states,  $(|\alpha\rangle \pm |-\alpha\rangle)/\sqrt{N_{\pm}}$ , which we refer to as the even and odd coherent state qubits (CSQ) [8–15]. Such a transformation can be performed probabilistically using the circuit shown in Fig. 1 (a). The gate is based on a supply of coherent state superposition resources which are assumed to have the same amplitude as the coherent states of the computational basis. The gate works by displacing the arbitrary CSQ input state  $|\psi_{\text{in}}\rangle = (u|\alpha\rangle + v|-\alpha\rangle)/\sqrt{N}$  followed by a joint but biased subtraction of a single photon from either the displaced input state or the resource

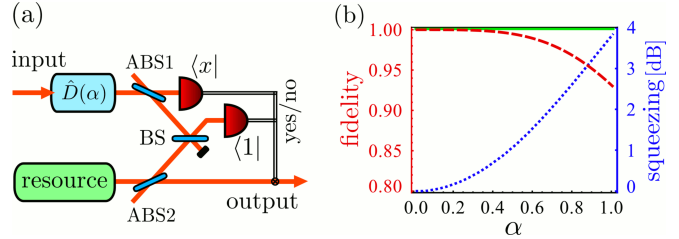


FIG. 1. (Color online) (a) Schematic of the Hadamard gate. The input coherent state qubit (CSQ) is displaced ( $\hat{D}$ ) and mixed with a resource state at a beam splitter (BS). The output of the gate is conditioned by a single photon detection ( $\langle 1 \rangle$ ) and a homodyne measurement ( $\langle x \rangle$ ). (b) Gate fidelity as a function of the CSQ amplitude for an ideal coherent state superposition resource (solid green) and the squeezed state resource (dashed red). The degree of squeezing that optimizes the fidelity is represented by the dotted blue curve.

state. Physically, this can be done by reflecting a small part of either state using highly asymmetric beam splitters (ABS1,ABS2), interfering the resulting beams on a beam splitter (BS) with transmittivity  $t$  and reflectivity  $r$ , and detecting one photon at the output with a single-photon detector. Theoretically this is described by the operator  $r\hat{a} + t\hat{b}$  where  $\hat{a}$  and  $\hat{b}$  are annihilation operators corresponding to the subtraction of a photon from the displaced input and the coherent state superposition resource, respectively. As a final step the two-mode state is projected onto the single-mode quadrature eigenstate  $|x\rangle$ , where  $x$  is the amplitude quadrature, by using a homodyne detector (HD). The resulting output state is

$$u\frac{|\alpha\rangle + |-\alpha\rangle}{\sqrt{N_+}} + Y_1(u+vZ)\frac{|\alpha\rangle - |-\alpha\rangle}{\sqrt{N_-}}, \quad (1)$$

where

$$Y_1 = \frac{t}{2r}\sqrt{\frac{N_-}{N_+}}, \quad Z = \frac{\langle x|0\rangle}{\langle x|2\alpha\rangle}. \quad (2)$$

By using a beam splitter (BS) with  $t \ll r$  and setting the  $x$  quadrature such that  $Z \gg 1$  and  $ZY_1 = 1$ , the Hadamard transform is implemented. The gate is probabilistic, and implemented by a hybrid detection system, using both discrete and continuous variable projections [16, 17]. Its success is conditioned on the joint measurement of a photon and a quadrature measurement outcome with the value  $x$ .

As an even coherent state superposition with small amplitude is reminiscent of a squeezed vacuum state, and this latter state is experimentally easier to prepare, we will in the following consider the replacement of the ideal resource with a squeezed vacuum state. With this substitution, the transformed state will have the following form,

$$u\hat{S}(s)|0\rangle + Y_2(u+vZ)\hat{S}(s)\hat{a}^\dagger|0\rangle, \quad (3)$$

where  $s$  is the squeezing parameter which is related to the squeezing variance by  $V = e^{-2s}$ , and the parameter  $Y_2$  is now given by

$$Y_2 = -t \sinh(s)/(2r\alpha). \quad (4)$$

Again, the requirement for optimal implementation of the Hadamard transform is  $Z \gg 1$  and  $ZY_2 = 1$ . Using this result we calculate the expected gate fidelity for various amplitudes  $\alpha$  as shown by the dashed red curve in Fig. 1 (b). For the squeezed vacuum resource, we optimize the squeezing degree (shown by the dotted blue curve) to obtain the highest fidelity which reaches unity for  $\alpha = 0$ . At higher amplitudes, the resource deviates from the ideal coherent state superposition and thus the fidelity decreases. For comparison, we also plot the expected gate fidelity for the case of an ideal resource (the solid green line). In the experiment described below we use  $\alpha = 0.8$  which gives a reasonable trade-off between fidelity

( $F = 0.97$ ), required squeezing ( $V = 2.6$  dB) and success probability.

The experimental setup is presented in Fig. 2. Nearly Fourier-limited picosecond pulses (4.6 ps) generated by a cavity dumped Ti:sapphire laser with repetition rate of 815 kHz and central wavelength of 830 nm are frequency doubled (SHG) by single passing a 3 mm long periodically poled KTiOPO<sub>4</sub> nonlinear crystal (PPKTP1). Up-converted pulses at 415 nm pumps a second crystal (PPKTP2) which is phase-matched for degenerate collinear optical parametric amplification (OPA), thus yielding squeezed vacuum of up to 3 dB of squeezing. This state is used as a resource for the Hadamard gate. An adjustable fraction of an orthogonally polarized mode at 830 nm passes the OPA crystal unchanged and serves as the input coherent state to the gate. About 7.5% and 1.5% of the coaxially propagating resource and input modes, respectively, are reflected off an asymmetric beam splitter (ABS) and transmitted through a half wave plate (HWP) and a polarizing beam splitter (PBS1) which in combination acts as a variable beam splitter (BS) thus mixing the input mode and the resource mode. The transmittance  $|t|^2$  of the BS is set to 25%. The output is spatially and spectrally filtered by a single mode optical fiber (SMF) and a narrow interference filter (IF) with a bandwidth of 0.05 nm and detected by a single photon counting module based on a silicon avalanche photo diode (APD) with dark count rate of  $20 \pm 4$  per second. The total efficiency of the APD arm reaches  $25 \pm 4\%$ .

The transmitted fraction of the modes after the asymmetric beam splitter is superimposed with a bright local oscillator (LO) at a polarizing beam splitter (PBS2). The amplitude quadrature is measured on the reflected mode by homodyne detection with a fixed relative phase set to zero. The recording of the measurement results was done by correlating the APD detection events with a synchronization signal from the laser cavity dumper through a coincidence circuit to decrease the probability of dark events. Every time a photon was detected by the APD within the accepted time slot, the homodyne signal was sampled by an oscilloscope running in memory segmentation regime and fed to a computer where the corresponding quadrature value was processed. The state at

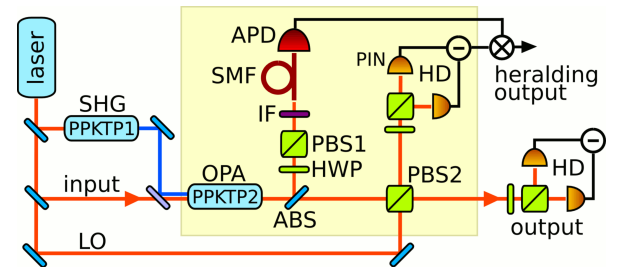


FIG. 2. (Color online) Experimental setup for the coherent state qubit Hadamard gate.

the output of the gate is measured with another homodyne detector with the relative phase of the LO scanned over a period and then reconstructed using maximum-likelihood based quantum state tomography [18] taking into account the total homodyne detection efficiency of  $77 \pm 2\%$ .

In our experiment, we investigated the performance of the Hadamard gate for the computational basis states  $|- \alpha\rangle$  and  $|\alpha\rangle$  as inputs. After the displacement operation,  $\hat{D}(\alpha)$ , this corresponds to the injection of  $|0\rangle$  and  $|2\alpha\rangle$ , where  $\alpha = 0.8 \pm 0.2$  in our case. The uncertainty is due to the imperfect calibration of total losses of the whole setup. As described, the gate is heralded by conditioning on two different measurement outcomes—the APD detection event and a certain outcome of the first homodyne detector. It can be seen that the conditional homodyning only plays a role when we inject a CSQ into the gate, i.e. when  $u, v \neq 0$ . With coherent states as the input, the solution is to choose a narrow heralding window that would balance the success probabilities of the gate for those basis states. For the input state  $|- \alpha\rangle$  the APD detection probability was of the order of  $10^{-3}$  while for the  $|\alpha\rangle$  input state, the probability was of the order of  $10^{-2}$ . From this we can see that we need to choose a heralding window that will balance out the factor of 10. Based on the experimental data we found its optimal position  $x = 0.4$  and the width of 0.02 that would give us an overall success probability of the order of  $10^{-5}$ .

The reconstructed output states for both input states  $|- \alpha\rangle$  and  $|\alpha\rangle$  can be seen in Fig. 3. For the  $|- \alpha\rangle$  input, the gate yields a state which closely resembles a

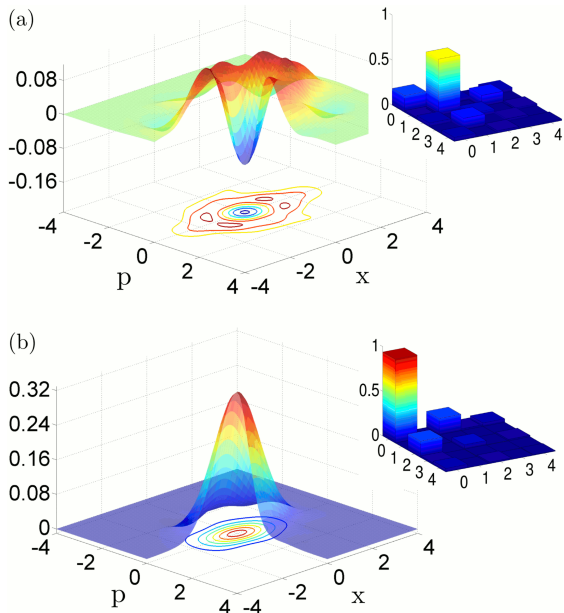


FIG. 3. Reconstructed density matrices (insets) and calculated Wigner functions of the output states for (a)  $|- \alpha\rangle$  input and (b)  $|\alpha\rangle$  input.

small odd cat state which is what we expect from the gate operation. We found the fidelity between the prepared state and the ideal CSQ,  $(|\alpha\rangle - |-\alpha\rangle)/\sqrt{N_-}$ , is maximized for  $\alpha = 0.75$  and reaches the value of  $F_{-\alpha} = 0.65 \pm 0.04$ . The non classicality of the superposition state produced by the Hadamard gate can be seen from the negativity of the corresponding Wigner function which is  $W(0,0) = -0.11 \pm 0.02$ . For the  $|\alpha\rangle$  input, the output state closely resembles a squeezed state, approximating a small even CSQ,  $(|\alpha\rangle + |-\alpha\rangle)/\sqrt{N_+}$ . The fidelity between the prepared state and the ideal CSQ for  $\alpha = 0.75$  was found to be  $F_\alpha = 0.94 \pm 0.02$ .

The experimental results shown in Fig. 3 only provide a partial test of the Hadamard gate. In order to evaluate its action on an arbitrary CSQ as the input, we conducted a numerical simulation of the gate taking into account all the important experimental imperfections, namely the realistic splitting ratios of ABS1, ABS2 and BS, losses in APD and HD channels, and the impurity of our resource squeezed state. The effect of APD false clicks was included as well, but found to be negligible.

Our simulation starts with an arbitrary qubit in the coherent state basis,  $|\psi_{\text{in}}\rangle$ , for which the global input state reads

$$\hat{\rho}_{\text{in}} = |\psi_{\text{in}}\rangle_1\langle\psi_{\text{in}}| \otimes |0\rangle_2\langle 0| \otimes |0\rangle_3\langle 0| \otimes \hat{\rho}_4^A, \quad (5)$$

where the subscripts are used to label the four participating modes and  $\hat{\rho}^A$  represents the density matrix of a squeezed thermal state used as the ancillary resource. The action of the gate can now be represented by a unitary evolution of the linear optical elements,  $\hat{U}$ , followed by POVM elements of successful heralding events  $\hat{\Pi}$ , with the output state given by

$$\rho_{\text{out}} = \frac{1}{P_S} \text{Tr}_{123}(\hat{U} \hat{\rho}_{\text{in}} \hat{U}^\dagger \hat{\Pi}), \quad (6)$$

where  $P_S = \text{Tr}(\hat{U} \hat{\rho}_{\text{in}} \hat{U}^\dagger \hat{\Pi})$  is the success rate.  $\hat{U} = \hat{U}_{23}(t_{\text{BS}}) \hat{U}_{12}(t_{\text{ABS1}}) \hat{U}_{34}(t_{\text{ABS2}})$  is composed of unitary beam splitter operations coupling the respective modes, and  $\hat{\Pi} = \hat{\Pi}_1^{\text{HD}} \otimes \hat{\Pi}_3^{\text{APD}}$  describes the inefficient homodyne and APD measurements. To parametrize a Bloch sphere of input CSQ states we denote  $u = \cos\theta$  and  $v = \sin\theta \exp(i\phi)$ , where  $\theta \in [0, \pi/2]$  and  $\phi \in [0, 2\pi]$ . The north and south poles correspond to the pseudo-orthogonal states  $|\alpha\rangle$  and  $|- \alpha\rangle$ , respectively. A mapping of this Bloch sphere onto the corresponding fidelities and success probabilities at the output is shown in Fig. 4. The fidelity spans the interval of  $F \in [0.67, 0.96]$  with the average value of  $\bar{F} = 0.78$ . Particularly, for coherent states  $|\alpha\rangle$  and  $|- \alpha\rangle$  at the input, the fidelities of 0.88 and 0.67 are predicted, respectively, which agrees well with the actually measured values. The success probabilities associated with  $|\alpha\rangle$  and  $|- \alpha\rangle$  are almost equal which confirms the correct value of the amplitude quadrature used at the HD for conditioning. The average success probability is  $\bar{P}_S = 7.2 \times 10^{-6}$ .

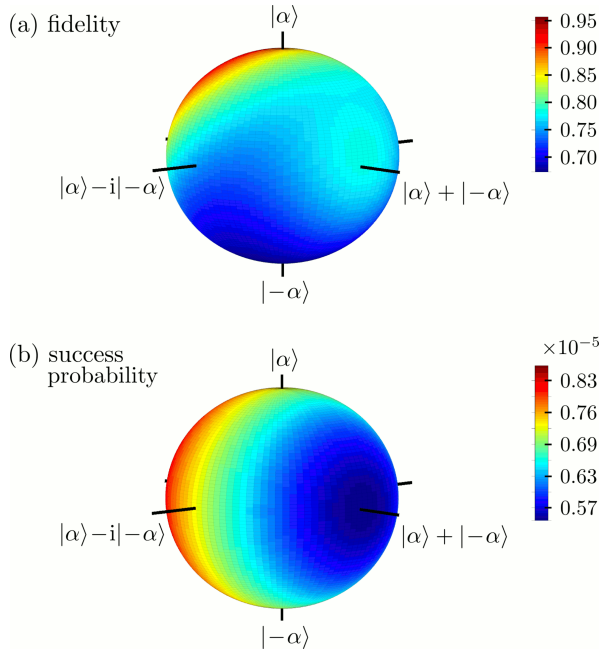


FIG. 4. The overall quality of the gate is visualized by mapping the Bloch sphere of input CSQ onto the fidelity  $F$  of the output states (a) and their corresponding success probabilities  $P_S$  (b).

Alternatively, we quantify the performance of the gate by employing the process fidelity. This quantity is based on the elegant notion that any operation can be implemented through teleportation: The desired operation is conducted onto an entangled state which is subsequently used to teleport the state on which the operation should be imparted [19]. The quality of such an operation is given by the quality of the actually transformed entangled state, which can be quantified by the fidelity with respect to the ideally transformed entangled state. We have performed a numerical simulation of the transformation of the entangled state  $|\alpha, \alpha\rangle + |-\alpha, -\alpha\rangle$  and compared it to the ideally transformed state,  $|\alpha\rangle(|\alpha\rangle + |-\alpha\rangle)/\sqrt{N_+ + |-\alpha\rangle(|\alpha\rangle - |-\alpha\rangle)/\sqrt{N_-}}$ . The process fidelity resulting from this simulation reaches  $\mathcal{F} = 0.70$ .

In conclusion, we have demonstrated a single mode Hadamard gate for coherent state qubits by using a hybrid projector system consisting of a conditional homodyne detector and a photon counter. This implementation constitutes the first step towards the demonstration of quantum computing with macroscopic qubit states. To implement universal quantum computing, the Hadamard gate must be supplemented with a single mode phase gate (a simplified version was recently implemented [20]) and a two-mode controlled phase gate. In addition to the implementation of these gates, another outlook is to refine the experimental techniques or propose new schemes that may increase the gate fidelity, and thus eventually may

allow for fault-tolerant operation.

The work was financed by the Danish Research Agency (Project No. FNU 09-072623) and EU project COMPAS. PM acknowledges the support by Projects No. ME10156 of the Czech Ministry of Education and No. P205/10/P319 of the Czech Grant Agency. MJ acknowledges the support by Projects No. MSM6198959213 and No. LC06007 of the Czech Ministry of Education and by the Palacký University (PrF\_2011\_015).

\* Corresponding author: anders.tipsmark@fysik.dtu.dk

- [1] P. Kok et al., Rev. Mod. Phys. **79**, 135 (2007).
- [2] R. Raussendorf, D. Browne, and H. Briegel, Phys. Rev. A **68**, 022312 (2003).
- [3] E. Knill, R. Laflamme, and G. Milburn, Nature **409**, 46 (2001).
- [4] T. Ralph et al., Phys. Rev. A **68**, 42319 (2003).
- [5] H. Jeong and T. Ralph, In: *Quantum Information With Continuous Variables of Atoms and Light*, edited by N.J. Cerf, G. Leuchs, and E.S. Polzik (Imperial College Press, 2007).
- [6] A. P. Lund et al., Phys. Rev. Lett. **100**, 030503 (2008).
- [7] P. Marek and J. Fiurášek, Phys. Rev. A **82**, 014304 (2010).
- [8] The Hadamard transform is the unitary operation defined as  $\hat{H}(x|0\rangle + y|1\rangle) \rightarrow x(|0\rangle + |1\rangle) + y(|0\rangle - |1\rangle)$ , assuming  $\langle 0|1\rangle = 0$ . In our case the coherent basis states  $|\alpha\rangle$  and  $|-\alpha\rangle$  are only approximately orthogonal which opens a question of the normalization of the corresponding CSQ states. Our choice of the normalized transformations (in contrast to  $|\pm\alpha\rangle \rightarrow |\alpha\rangle \pm |-\alpha\rangle$ ) has the benefit of all states being physically sound and, consequently, fidelities for  $\alpha \rightarrow 0$  approaching unity. On the other hand, it is true that for these small amplitudes the gate does not behave exactly as the Hadamard gate. However, this is a general problem caused by the non-orthogonality of the coherent states and we are avoiding it by choosing reasonably large  $\alpha$ . Furthermore, our gate implements both the transformations (the normalized as well as the unnormalized one), switching between them just by a suitable choice of the quadrature value used at the HD for heralding of the gate.
- [9] J.S. Neergaard-Nielsen et al., Phys. Rev. Lett. **105**, 053602 (2010).
- [10] J. Wenger et al., Phys. Rev. Lett. **92**, 153601 (2004).
- [11] J. S. Neergaard-Nielsen et al., Phys. Rev. Lett. **97**, 083604 (2006).
- [12] A. Ourjoumtsev, et al., Science **312**, 83 (2006).
- [13] K. Wakui et al., Optics Express **15**, 3568 (2007).
- [14] N. Namekata et al., Nature Photonics **4**, 655 (2010).
- [15] T. Gerrits, Phys. Rev. A **82**, 031802(R) (2010).
- [16] S.A. Babichev et al., Phys. Rev. Lett. **92**, 047903 (2004).
- [17] A. Ourjoumtsev, et al., Nature **448**, 784 (2007).
- [18] Z. Hradil, Phys. Rev. A **55**, R1561 (1997); M. Ježek et al., Phys. Rev. A **68**, 012305 (2003); A.I. Lvovsky, J. Opt. B: Quant. Semiclass. Opt. **6**, S556 (2004).
- [19] D. Gottesman and I. L. Chuang, Nature **402**, 390 (1999); L. Slodička et al., Phys. Rev. A **79**, 050304(R) (2009).
- [20] R. Blandino et al., quant-ph arXiv:1105.5510 (2011).